

Model-based projections of Zika virus infections in childbearing women in the Americas

T. Alex Perkins^{1*}, Amir S. Siraj¹, Corrine Warren Ruktanonchai², Moritz U.G. Kraemer³,
Andrew J. Tatem^{2,4}

¹ Department of Biological Sciences and Eck Institute for Global Health, 100 Galvin Hall,
University of Notre Dame, Notre Dame, IN 46556 USA

² WorldPop, Department of Geography and Environment, University of Southampton,
Southampton, SO17 1BJ, UK

³ Spatial Ecology and Epidemiology Group, Department of Zoology, University of Oxford,
Oxford, OX1 3PS, UK

⁴ Flowminder Foundation, Stockholm, Sweden

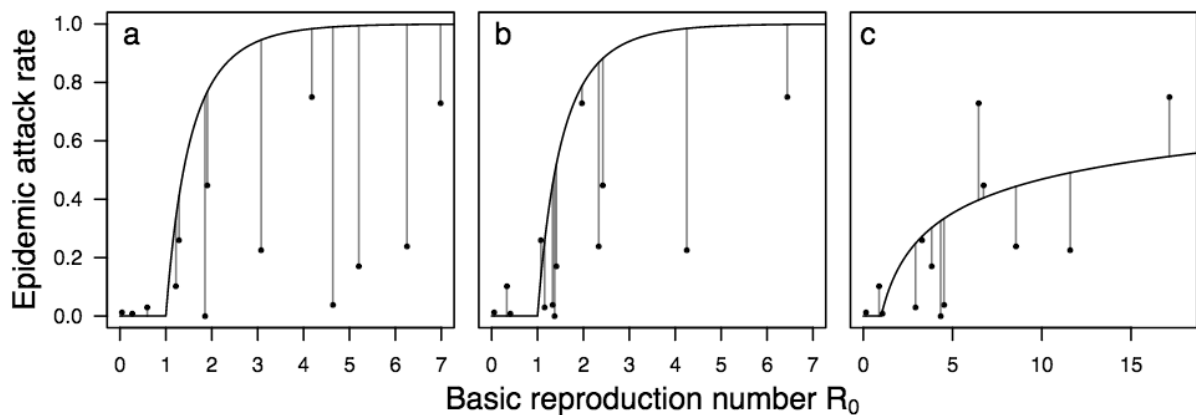
* Author for correspondence: taperkins@nd.edu

Supplementary Table 1. Seroprevalence estimates for Zika and chikungunya viruses in the context of recent outbreaks in a previously susceptible population.

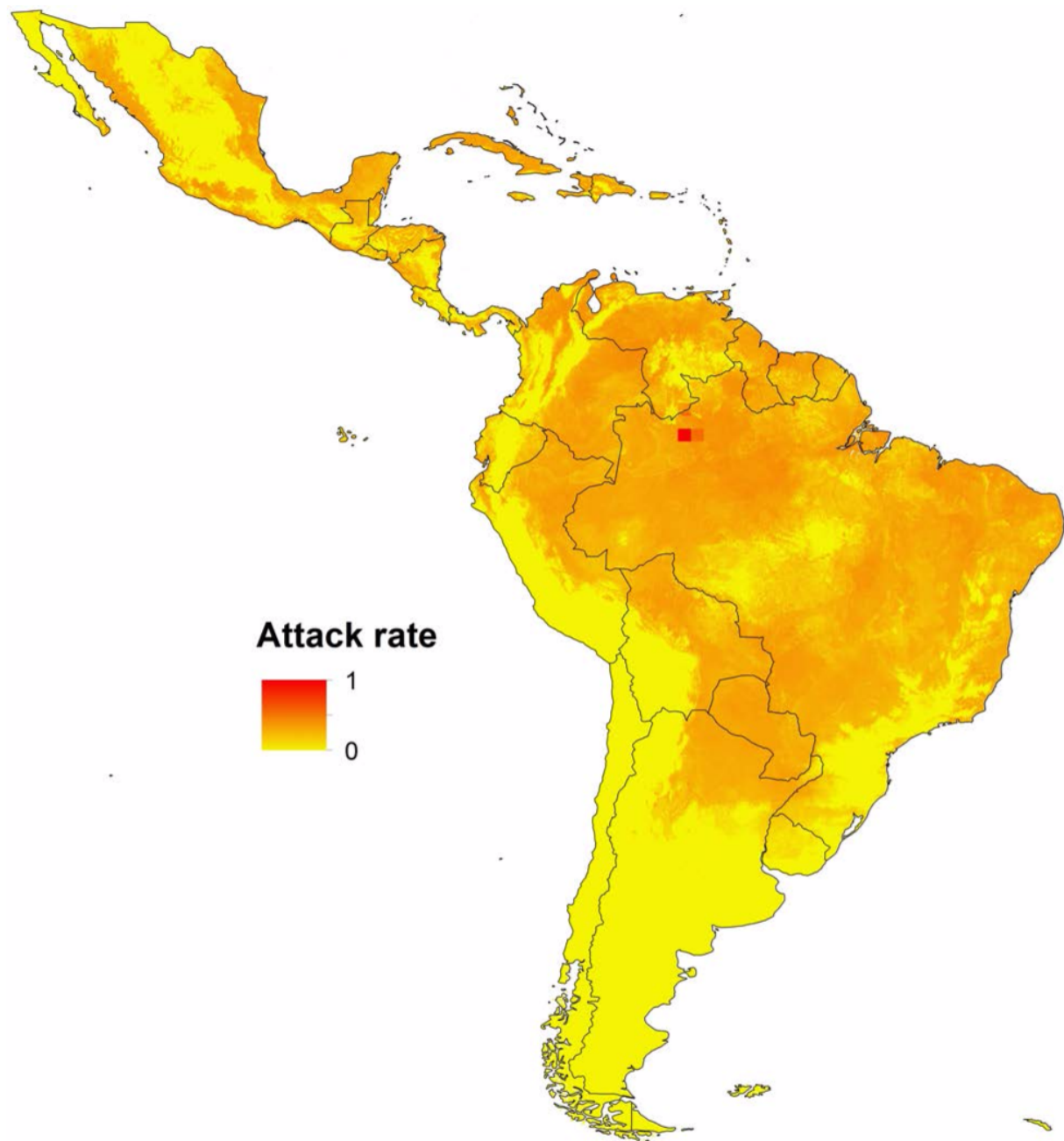
Seroprevalence	Virus	Location	Reference
0.75	CHIKV	Lamu Island, Kenya	15
0.73	ZIKV	Yap Island, Federated States of Micronesia	49
0.446	CHIKV	Mananjary, Madagascar	50
0.26	CHIKV	Mayotte Island, Union of the Comoros	51
0.24	CHIKV	Orissa, India	52
0.227	CHIKV	Manakara, Madagascar	50
0.169	CHIKV	Saint Martin	53
0.103	CHIKV	Emilia-Romagna, Italy	54
0.039*	CHIKV	Managua, Nicaragua	55
0.031	CHIKV	Moramanga, Madagascar	50
0.011	CHIKV	Ambositra, Madagascar	50
0.01	CHIKV	Ifanadiana, Madagascar	50
0.0	CHIKV	Tsiroanomandidy, Madagascar	50

* This estimate was based on a clinical attack rate of 0.029 and an assumed reporting rate of 0.75.

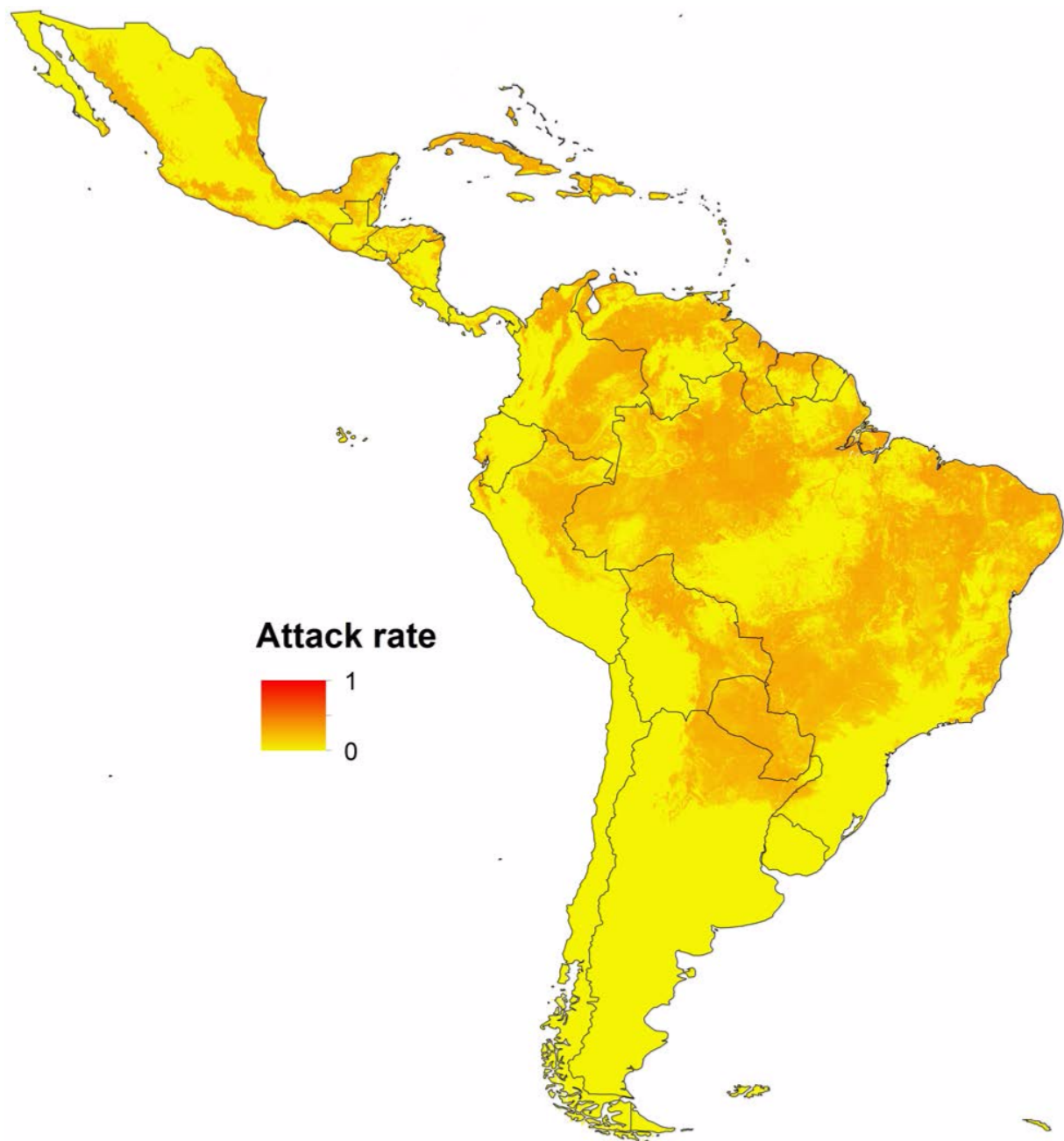
Supplementary Figure 1. Relationships between the basic reproduction number R_0 (x-axis) and epidemic attack rates (y-axis) under different model assumptions (a-c). In each panel, the curve shows this relationship under a given set of model assumptions and the points represent the 13 seroprevalence estimates (Supplementary Table 1) mapped on to the R_0 -axis based on conditions at the sites where those data were collected. (a) R_0 calculations according to eqn. 1 under the assumption that $m = 1$ and with parameter $\alpha = 1$ determining the shape of the curve. (b) R_0 calculations according to eqn. 1 under the assumption that m is determined by a SCAM model of the economic index and with parameter $\alpha = 1$. (c) Same as b but with parameter $\alpha = 0.13$ fitted by least squares and a separate SCAM model fitted conditional on α .



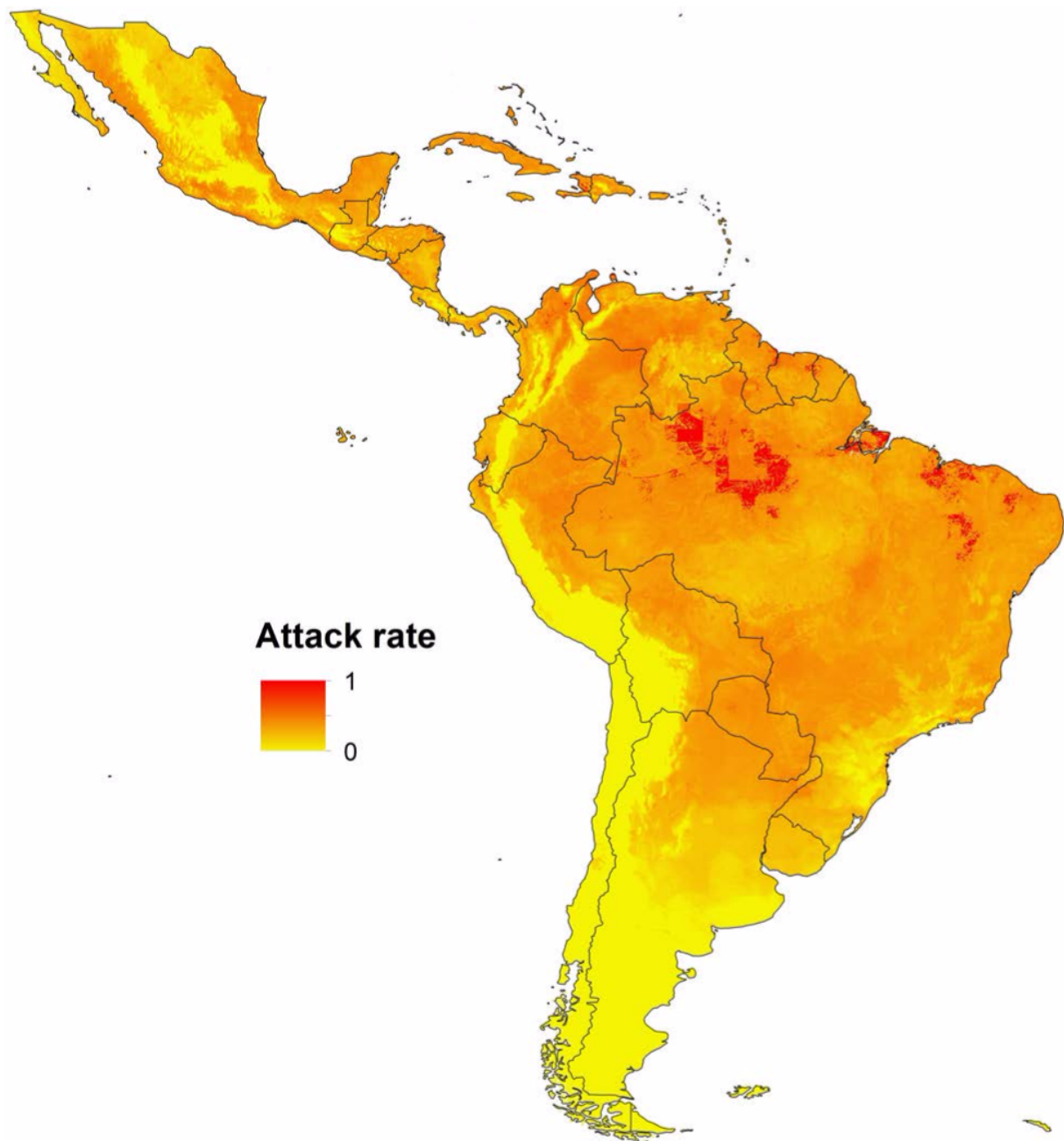
Supplementary Figure 2. Gridded spatial projections of median epidemic attack rates at 5x5 km resolution in Latin America and the Caribbean. Each grid cell is shaded according to the median epidemic attack rate for that grid cell from the distribution of 1,000 Monte Carlo samples.



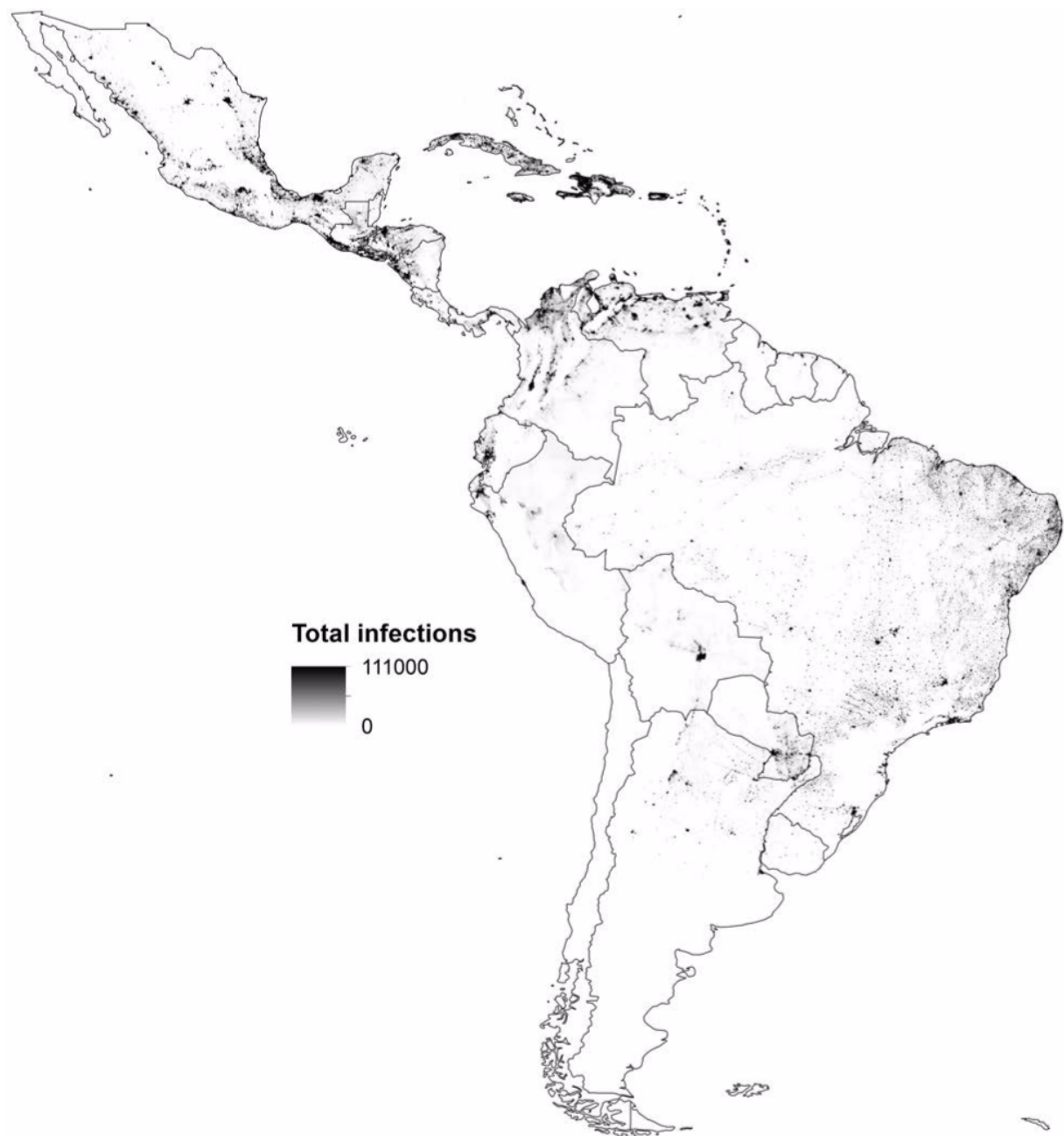
Supplementary Figure 3. Gridded spatial projections of minimum epidemic attack rates at 5x5 km resolution in Latin America and the Caribbean. Each grid cell is shaded according to the minimum epidemic attack rate for that grid cell from the distribution of 1,000 Monte Carlo samples.



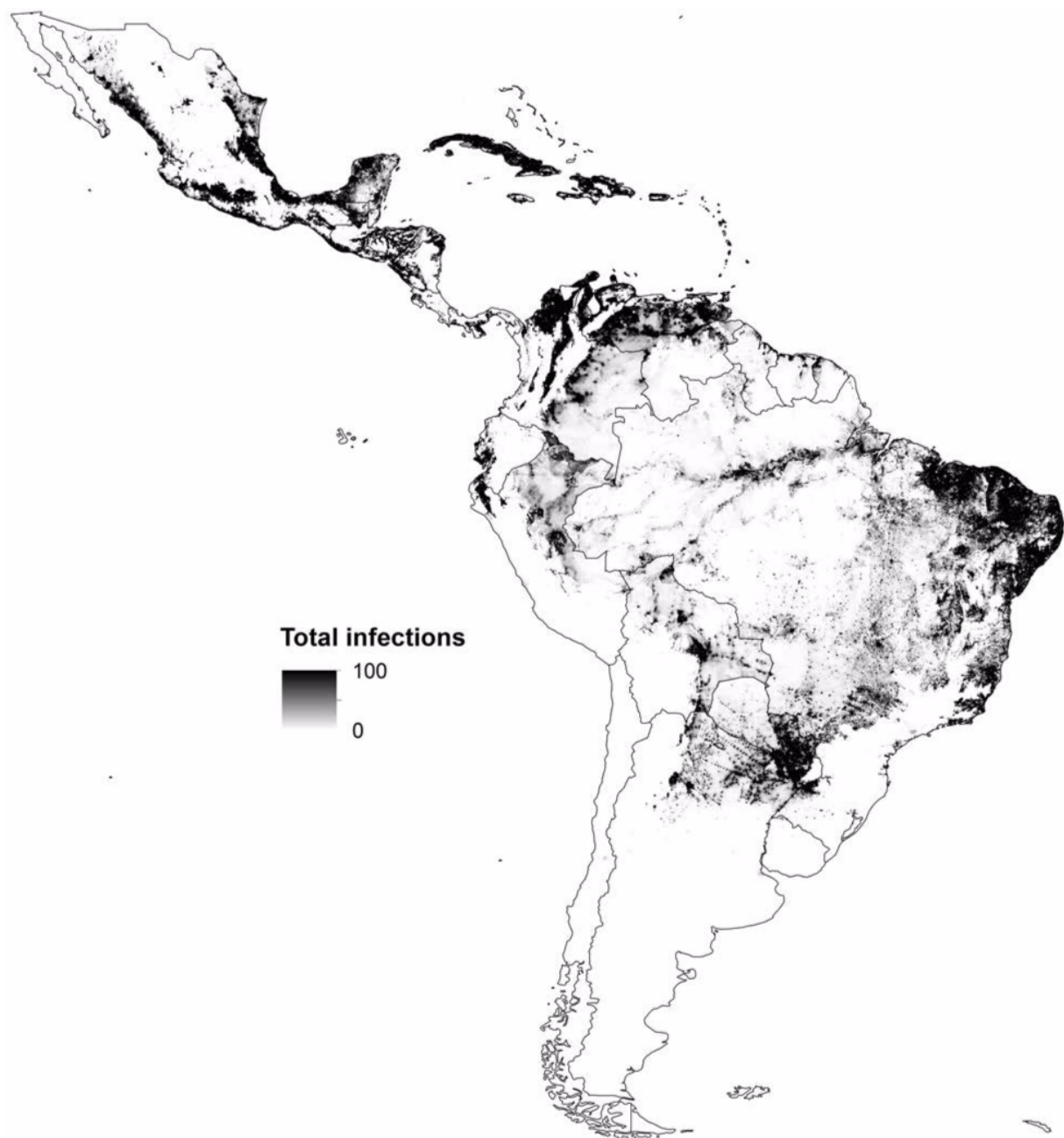
Supplementary Figure 4. Gridded spatial projections of maximum epidemic attack rates at 5x5 km resolution in Latin America and the Caribbean. Each grid cell is shaded according to the maximum epidemic attack rate for that grid cell from the distribution of 1,000 Monte Carlo samples.



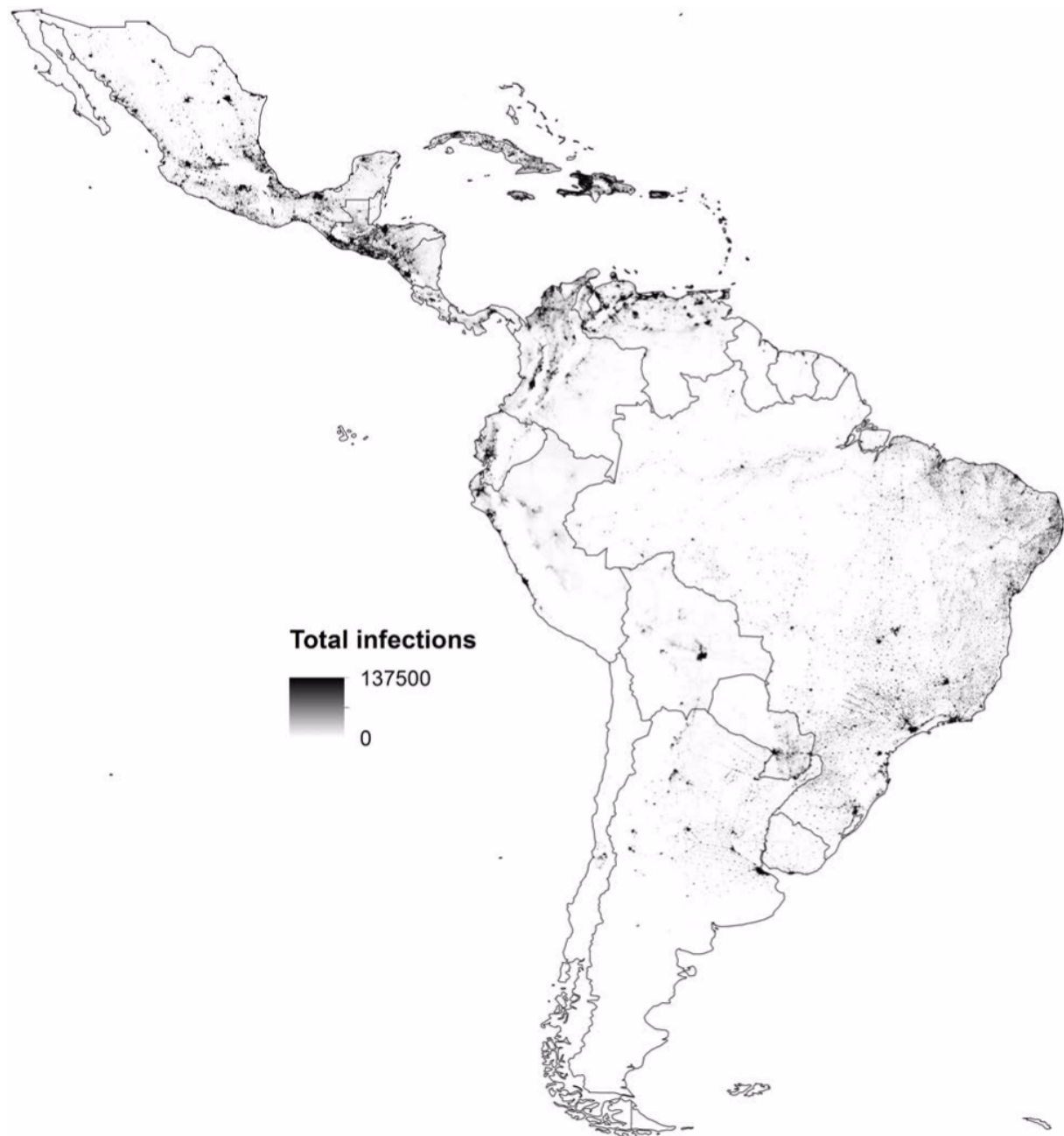
Supplementary Figure 5. Gridded spatial projections of median infections among the total population at 5x5 km resolution in Latin America and the Caribbean. Each grid cell is shaded according to the median number of infections for that grid cell from the distribution of 1,000 Monte Carlo samples.



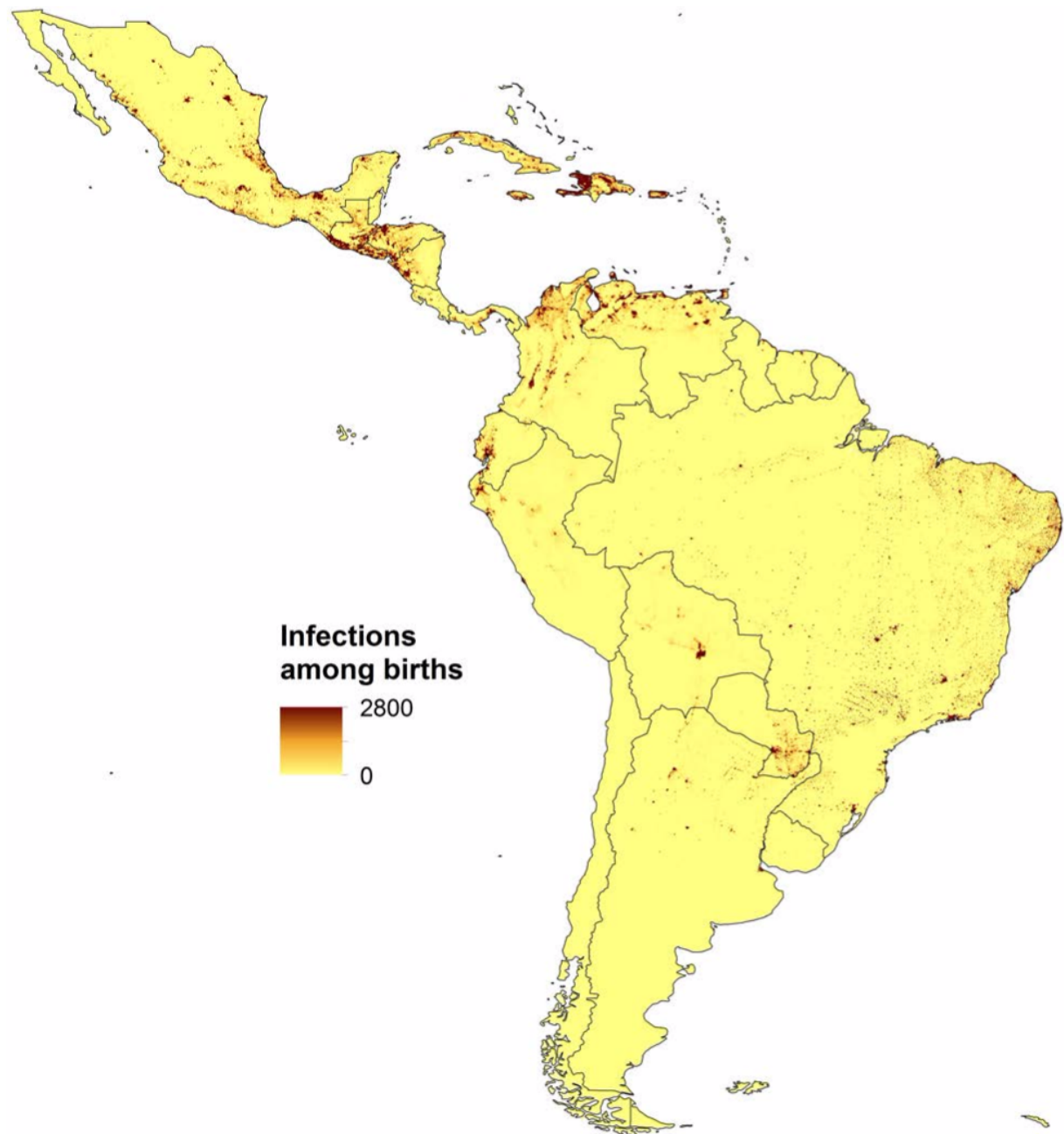
Supplementary Figure 6. Gridded spatial projections of minimum infections among the total population at 5x5 km resolution in Latin America and the Caribbean. Each grid cell is shaded according to the minimum number of infections for that grid cell from the distribution of 1,000 Monte Carlo samples.



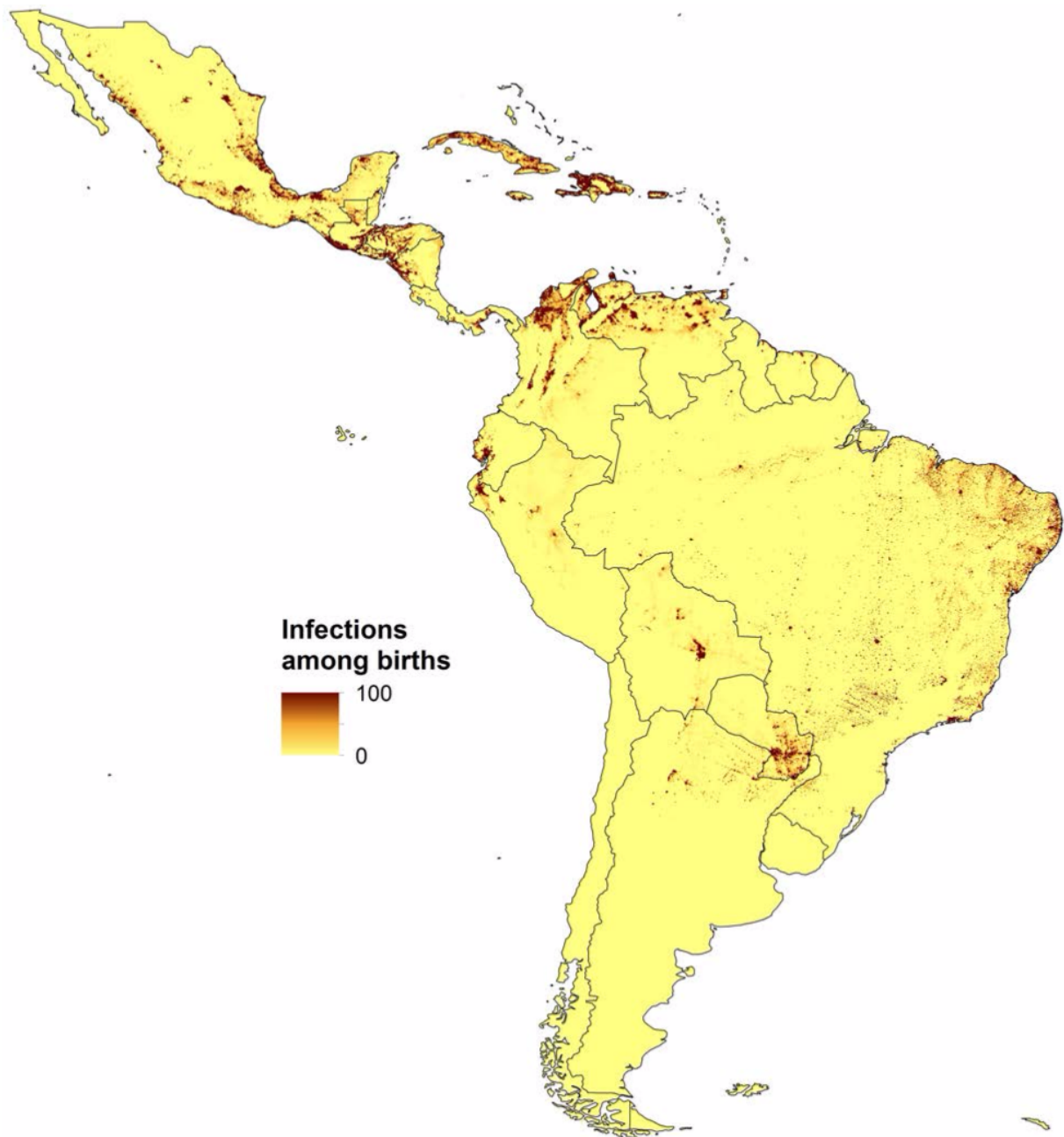
Supplementary Figure 7. Gridded spatial projections of maximum infections among the total population at 5x5 km resolution in Latin America and the Caribbean. Each grid cell is shaded according to the maximum number of infections for that grid cell from the distribution of 1,000 Monte Carlo samples.



Supplementary Figure 8. Gridded spatial projections of median infections among childbearing women at 5x5 km resolution in Latin America and the Caribbean. Each grid cell is shaded according to the median number of infections for that grid cell from the distribution of 1,000 Monte Carlo samples.



Supplementary Figure 9. Gridded spatial projections of minimum infections among childbearing women at 5x5 km resolution in Latin America and the Caribbean. Each grid cell is shaded according to the minimum number of infections for that grid cell from the distribution of 1,000 Monte Carlo samples.



Supplementary Figure 10. Gridded spatial projections of maximum infections among childbearing women at 5x5 km resolution in Latin America and the Caribbean. Each grid cell is shaded according to the maximum number of infections for that grid cell from the distribution of 1,000 Monte Carlo samples.

